Advanced LIGO laser systems for O3 and future observation runs

Nina Bode [1],* [iD] **, Joseph Briggs** [2] [iD] **, Xu Chen** [3] **, Maik Frede** [4] **, Peter Fritschel** [5] **, Michael Fyffe** [6] **,
Eric Gustafson** [7] **, Matthew Heintze** [6] **, Peter King** [8] **, Jian Liu** [1] **, Jason Oberling** [9] **, Richard Savage** [9] **,
Andrew Spencer** [2] [iD] **and Benno Willke** [1] [iD]

[1]   Max Planck Institute for Gravitational Physics (Albert Einstein Institute) and Institute for Gravitational
      Physics and Leibniz University Hannover, Callinstrasse 38, D-30167 Hannover, Germany
[2]   SUPA, University of Glasgow, Glasgow G12 8QQ, United Kingdom
[3]   OzGrav, University of Western Australia, Crawley, Western Australia 6009, Australia
[4]   neoLASE GmbH, Hollerithallee 17, 30419 Hannover, Germany
[5]   LIGO, Massachusetts Institute of Technology, Cambridge, MA 02139, United States of America
[6]   LIGO Livingston Observatory, Livingston, LA 70754, United States of America
[7]   LIGO Laboratory, California Institute of Technology, Pasadena, CA 91125, United States of America
[8]   California Institute of Technology, Pasadena, CA 91125, United States of America
[9]   LIGO Hanford Observatory, Richland, WA 99352, United States of America
*   Correspondence: nina.bode@aei.mpg.de

1   **Abstract:** The advanced LIGO gravitational wave detectors need high power laser sources with an
2   excellent beam quality and a low noise behaviour. We present the pre-stabilized laser system with
3   70 W of output power that was used in the third observing run of the advanced LIGO detectors.
4   Furthermore, the prototype of a 140 W pre-stabilized laser system for future use in the LIGO
5   observatories is described and characterized.

6   **Keywords:** pre-stabilized laser system; neoVAN-4S; neoVAN-4S-HP

---

7   ## 1. Introduction

8   The advanced LIGO (aLIGO) gravitational wave detectors [1] are the most sensitive optical
9   measurement systems in the world. Built as Michelson interferometers with arm lengths of several
10   kilometers they can detect gravitational waves that cause arm length changes below 10^{-19}m. The
11   sensitivity of these detectors is determined by several parameters, such as the laser power, the
12   interferometer arm length, mirror quality and seismic isolation.
13   A crucial part in these interferometers is the laser system and its stabilization. The requirements on the
14   laser system is given by its influence on the detectors sensitivity. At high frequencies, the detector's
15   sensitivity is limited by photon shot noise that couples with $1/\sqrt{P}$, hence a high laser power P is
16   needed. The aLIGO gravitational wave detectors are operated with the so called DC readout [2]. That
17   means that the output sensor always detects a small amount of laser power. Thus, laser power noise
18   couples directly in the interferometer readout and has to be as low as possible. Also pointing noise
19   leaks into the interferometer output due to misalignment on the modecleaners and the beam splitter.
20   Laser frequency noise couples whenever the arms are not of equal length or the Fabry Pérot cavities
21   in the interferometer arms are asymmetric. The mode purity of the laser beam that is sent to the
22   interferometer determines the power inside the interferometer as well as the shot noise on length and
23   alignment sensors. Thus the mode purity has to be as high as possible. This is typically achieved by
24   spatial beam filtering via a pre-modecleaner and an input-modecleaner, but to preserve as much power
25   from the initial laser beam as possible a good mode quality should be provided from the beginning.

26 The combination of a high power laser beam with high spatial beam quality and stability is needed to
27 operate a gravitational wave detector with high sensitivity.
28 In the first section of this paper we present the setup and performance of the pre-stabilized laser system
29 (PSL) that was used in the last observing run of aLIGO (O3). This laser system operated at an output
30 power of 70 W and a wavelength of 1064 nm. It consisted of components that were installed already
31 for the two first aLIGO observation runs, with the addition of a new laser power amplifier.
32 The second section is devoted to the PSL that will be used for the next observing run (O4). The
33 O4 system will deliver twice the output power than the O3 system with a new amplification setup.
34 The pre-stabilization components will basically stay the same, but modifications in the intensity
35 stabilization electronics will be performed. A first prototype of this system was setup during O3 and
36 this paper presents the results of its characterization.
37 The O4 laser system section will be followed by a summary and an outlook towards possible laser
38 configurations for further upgrades of the aLIGO detectors in the end of this paper.

39 **2. Pre-stabilized laser system in O3**

40   The original laser power requirement to reach the aLIGO design sensitivity was 180 W at a
41 wavelength of 1064 nm before spatial filtering by the modecleaners[3] . The pre-stabilized laser system
42 that was designed to fulfill this requirements is described in [4]. It was based on a high power oscillator
43 (HPO) configuration [5], which was seeded by a non-planar ring oscillator laser (NPRO) [6] amplified
44 to 35 W by a medium power solid state amplifier [7] that was designed for and already used in the
45 enhanced LIGO (eLIGO) interferometers [8]. The combination of the NPRO and medium power
46 amplifier will be referred to as front-end. The HPO consisted of four neodymium doped crystals
47 as active medium, arranged in a ring configuration. High power pump diodes had to be used, to
48 compensate the low amplification efficiency. Thus, water cooling with high flow and big tubes was
49 necessary. Pointing noise caused by vibrations from this cooling had an unexpectedly high negative
50 influence on the interferometer. Based on this and the high maintenance effort associated with the
51 HPO it was decided to replace the oscillator with a much simpler solid state amplifier which was
52 integrated and tested in an aLIGO PSL reference environment at the Albert Einstein Institute (AEI) in
53 Hannover, Germany, before the installation at the LIGO observatories.
54 In the first part of this section we will describe the setup of the aLIGO O3 laser system based on these
55 amplifiers. This is followed by a characterization of the system and its performance during the O3
56 observation run.

57 *2.1. Setup*

58   The aLIGO PSL for O3 consisted of components that were already used in earlier observation
59 runs combined with a new amplification module. In Figure 1 a simplified setup of the laser system,
60 including the important parts for the pre-stabilization and characterization, is shown. For the seed
61 system an eLIGO front-end was used. This consists of a 2 W NPRO laser which seeds a solid state
62 amplifier consisting of four sequentially arranged water-cooled $Nd:YVO_4$ crystals that are pumped
63 with fiber coupled pump-diodes at a wavelength of 808 nm. An electro-optic modulator (EOM1) and a
64 Faraday isolator (FI1) are installed between the NPRO and the medium power amplifier. The front-end
65 delivered a maximal output power of 35 W that was sent through a second Faraday isolator (FI2) which
66 protected the front-end laser from back scattered and back reflected light.
67 A small amount of the front-end light transmitted by the FI2 was injected to a diagnostic breadboard
68 (DBB) [9,10]. This is a fully automated tool developed to measure the relative power noise (RPN),
69 frequency noise, relative beam pointing noise and higher order mode content of a laser beam. It is
70 based on a three mirror cavity which can be stabilized to the incident laser beam's frequency via a
71 dither locking scheme. The amplitude spectral density (ASD) of the control and error signals of this
72 feedback control loop can be combined to derive the frequency noise of the laser beam. By scanning
73 the cavity length and measuring the power in transmission of the cavity, a mode scan measurement
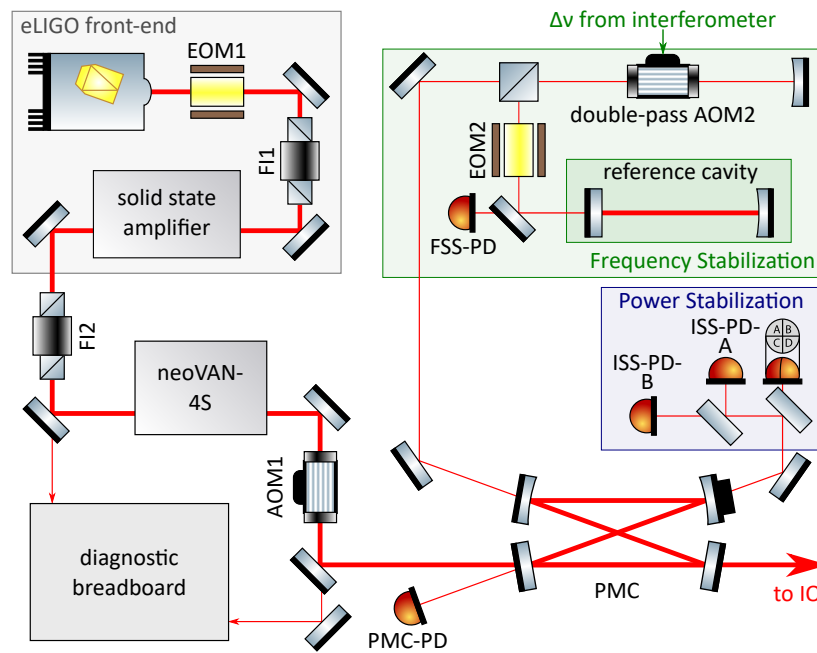
Figure 1. Simplified setup of the aLIGO O3 pre-stabilized laser system. An eLIGO front-end seeded the neoVAN-4S amplifier with an output power of 70 W. The main beam was sent through the PMC and then to the interferometer's input optics. The two low power output beams from the PMC were used for the frequency and power pre-stabilization stages.

74 can be performed that gives information about the higher order mode content compared to the TEM_{00}
75 eigenmode of the cavity. Automatic alignment of the incoming beam to the cavity eigenmode is
76 achieved by a differential wave front sensing scheme [11]. To implement the differential wave front
77 sensing, two piezo-electrically actuated mirrors and two quadrant photodiodes (QPD) are integrated
78 into the DBB. The error and control signal ASDs of the auto-alignment feedback control loops represent
79 the relative beam pointing noise of the incoming laser beam. A pick-off beam before the DBB cavity is
80 used to measure the relative power noise of the beam.
81 The front-end output was used to seed a neoVAN-4S solid state amplifier. This amplifier is similar to
82 the one in the front-end and consists of four Nd:YVO_4 crystals in series which are pumped with fiber
83 coupled pump diodes at a wavelength of 808 nm. The neoVAN-4S head and diodes are water-cooled
84 and the amplifier delivered an output power of 70 W.
85 The amplified laser beam was sent through an acousto-optic modulator (AOM1) to the bowtie
86 pre-modecleaner (PMC) which acts as a filter for the spatial beam profile and pointing noise of
87 the laser beam. Furthermore, the PMC filters power noise in the radio frequency range. The PMC that
88 was used at the Livingston site, was the same as used in earlier observation runs [12]. In Hanford the
89 all-bolted PMC, which is an updated version that has mechanically fastened mirrors instead of glued
90 ones, was installed for O3. The aim of this change was to avoid potential mirror contamination from
91 the glue, ease the fabrication process and allow an easy mirror swap if necessary [13]. The filtered
92 beam was then sent to the input optics subsystem (IO) [14].
93 The two low power output beams of the PMC were used for the frequency and power pre-stabilization
94 of the main laser beam. The frequency pre-stabilization was based on the reference cavity that was
95 used for the original aLIGO PSL. The reference cavity is a monolithic, linear, fused silica resonator
96 that is located inside an ultra-high vacuum chamber with a pressure below 10^{-6}Pa. It has a length
97 of 203 mm, a finesse of 11500 and is suspended by a single pendulum stage supported by a passive
98 vibration isolation stack. The laser beam was frequency stabilized to this ultra stable cavity via the
99 Pound-Drever-Hall locking scheme [15]. The required phase modulation side bands were imprinted
100 with EOM2. The FSS-PD photodiode signal was used to generate the control loop's error signal. The

101 control signal produced by the feedback control electronics was then sent to a piezoelectric element
102 attached to the NPRO laser crystal, the NPRO crystal temperature control and to EOM1. The complete
103 frequency stabilization loop of the gravitational wave detector consisted of more layers with the
104 long interferometer arms as final frequency reference. The double passed AOM2 was used to add a
105 frequency offset to the beam sent to the reference cavity. With this offset a stabilization of the main PSL
106 beam to the final reference is possible without changing the reference cavity length.
107 To pre-stabilize the laser's power, a set of an in-loop and out-of-loop photodiodes (ISS-PD-A and
108 ISS-PD-B) as well as a QPD (ISS-QPD) was setup in the second low power output port of the PMC. The
109 in-loop photodiode sensed the laser power, which was then compared to an electronic reference value
110 and amplified in the power stabilization electronic. The resulting control signal was sent to AOM1
111 which actuated on the laser power. AOM1 required an offset to enable an actuation towards higher
112 and lower laser powers. The complete power stabilization system contained a second loop which used
113 an additional photodiode behind the interferometer's input modecleaner as in-loop sensor and fed
114 back the control signal to the first loop's error point.
115 The pre-stabilized laser systems were the same for both aLIGO gravitational wave detectors. The laser
116 system was located in an isolated laser room and could be remotely operated via the LIGO control
117 and data system (CDS) [16]. All front-end and neoVAN-4S pump diodes and power supplies were
118 located in another room to prevent electro magnetic interference between the diode drivers and the
119 sensitive electronics located in the laser room. The electronics for the DBB, the PMC and the power
120 stabilization as well as the frequency stabilization CDS interface were located outside but close to the
121 laser room. Only the table top frequency stabilization servo (TTFSS) was located in the laser room, to
122 keep the distance to the actuators and with that the cable lengths as short as possible. The water chiller
123 for the front-end diodes and amplifier as well as the neoVAN-4S amplifier, diodes and electronics
124 was situated in the additional room to decrease the coupling between the laser system and vibrations,
125 acoustic noise and air flow generated by the chiller.
126 The laser power that finally was sent to the interferometer was adjusted with a half wave plate
127 followed by two thin film polarizers. The unit was part of the input optics and installed as one of the
128 last components in the laser room.

129 *2.2. Characterization and performance during O3*

130 A detailed description and characterization of a neoVAN-4S integrated in an aLIGO laser reference
131 system at the Albert Einstein Institute in Hannover (AEI) can be found in [17].
132 Here we present a set of DBB measurements that characterize the aLIGO O3 laser system in Livingston,
133 Louisiana, as well as a long term power trend measured in Hanford, Washington.
Figure 2b shows modescan measurements of the front-end beam and the output of the neoVAN-4S.
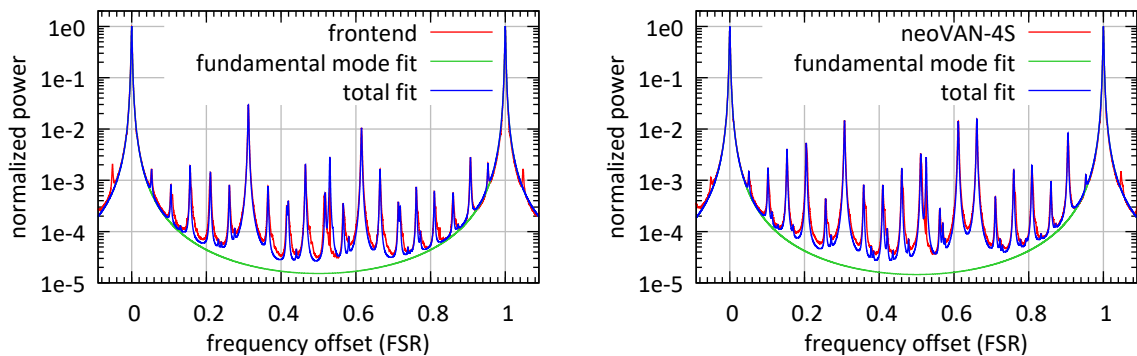

Figure 2. (a) Modescan of the laser beam coming from the front-end. The higher order mode content of
the laser beam was < 5.7%. (b) DBB modescan of laser beam amplified by the neoVAN-4S. The higher
order mode content of the laser beam was < 6.2%.

134 The peaks at zero and at one free spectral range (*FSR*) of the non-degenerated cavity are the TEM_{00}
135 peaks. The contribution of all higher order mode peaks in between the two shown TEM_{00} peaks
136 sum up to the laser beam's higher order mode content (HOM). The HOM calculated this way must
137 be understood as an upper limit for the laser beam's mode mismatch compared a perfect TEM_{00}
138 mode, as alignment and mode matching errors as well as imperfections of the DBB cavity's eigenmode
139 contribute to this number as well.
140 The most prominent peak in both modescans is the one at about $0.3FSR$. This peaks represents the
141 second order TEM modes and can thus be explained by a mode matching error or astigmatism in the
142 laser beam. Fourth order TEM modes are represented by the peak at $0.62FSR$. A small decrease in
143 second order mode peak often leads to an increase in the fourth order mode peak, as it can be seen
144 between the two measurements. The peak at $0.65FSR$ represents the TEM_{10} mode. Its increases behind
145 the second neoVAN-4S-HP is due two a slight misalignment of the beam to the DBB. An increase in all
146 the small higher order mode peaks leads to an increased HOM behind the neoVAN-4S.
147 The HOM content measured for the beam coming from the front-end is $< 5.7\%$ and the one for the
148 beam amplified by the neoVAN-4S is $< 6.2\%$. This corresponds to about $66\,W$ in the TEM_{00} mode.
The RPN measured behind the front-end and the neoVAN-4S, respectively, is shown in Figure 3. The
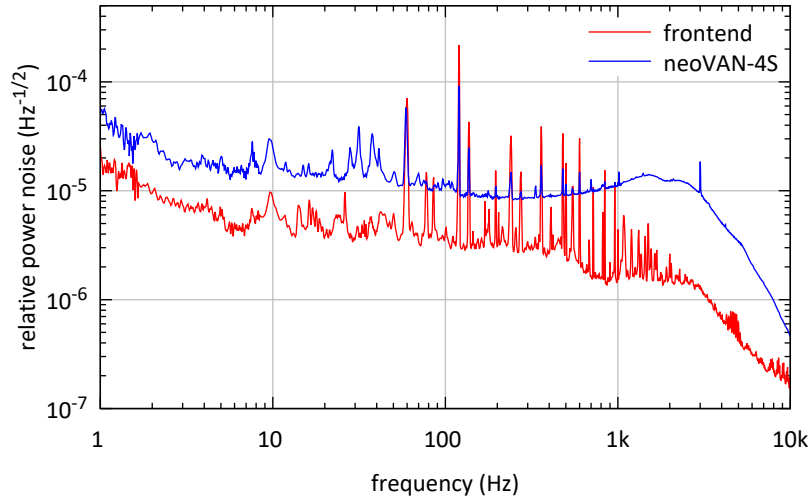

Figure 3. Relative power noise (RPN) measurements of the front-end laser beam and the laser beam amplified by the neoVAN-4S. The RPN is increased by the neoVAN-4S amplification. Measurements at the AEI Hannover showed that this is due to noise added by the pump diode power supplies.

149
150 RPN measured behind the neoVAN-4S is about four times higher than the front-end beam's RPN. This
151 measurement fits expectations generated from the AEI test setup. The RPN of the amplified beam is a
152 result of the uncorrelated sum from the seed's and the pump diode's noise contributions. The noise
153 contribution of the pump diodes was affected by the high noise of its pump diode power supplies as
154 already reported in [17].
155 Relative beam pointing measurements of the front-end beam and the output of the neoVAN-4S are
156 shown in Figure 4. Each curve represents the mean of four measurements, one for each degree of
157 freedom, which are depicted in a lighter version of the same color. Two degrees of freedom for the
158 relative beam pointing measurement are here defined as the lateral shift between the measured beam
159 and the reference beam, in this case the DBB cavity's eigenmode, at the location of the Gaussian beam
160 waist normalized by the waist radius $\delta x / w_0$ in vertical and horizontal direction. The other two degrees
161 of freedom are defined by a tilt between the measured beam and the same reference beam normalized
162 by the divergence angle of the Gaussian beam $\delta \alpha / \theta_D$, also in vertical and horizontal direction. The
163 two curves shown in figure 4 are very close to each other, which means that no additional pointing is
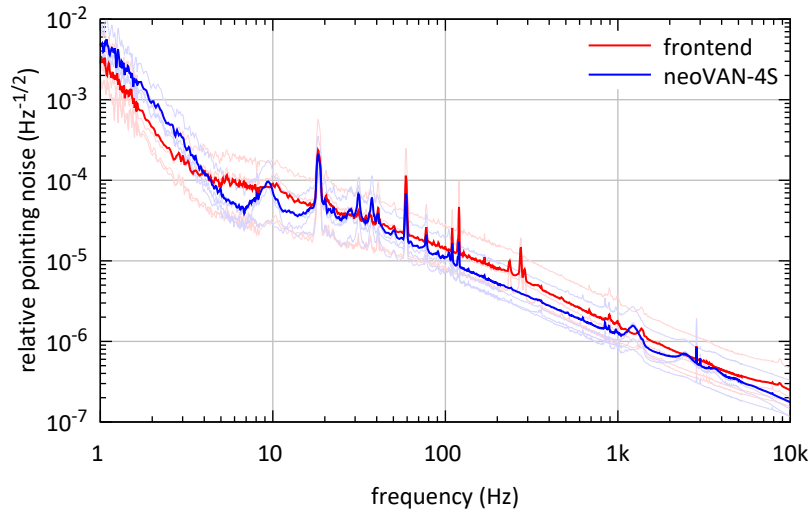164 generated by the neoVAN-4S.

Figure 4. Relative pointing measurements of the front-end laser beam and the laser beam amplified by the neoVAN-4S. The two curves are each representing the mean values of the four lighter curves in the same colour that show the measurement of the four alignment degrees of freedom for each laser. The relative pointing noise is not increased by the neoVAN-4S.

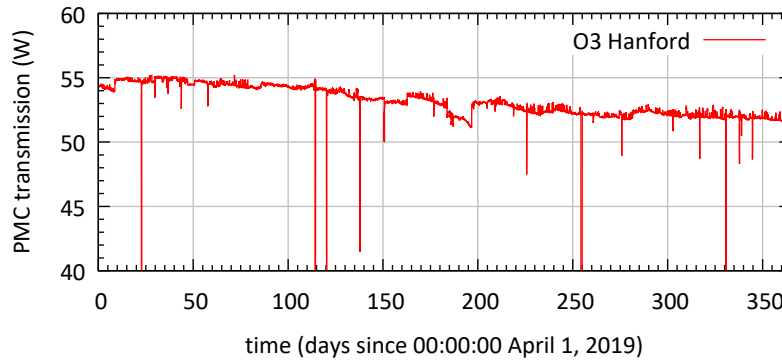In order to not miss a gravitational wave event during the observation run, the aLIGO laser system

Figure 5. The power transmitted by the PMC at the LIGO site in Hanford. The system was available the whole observation run. The total power decreased over time from 55 W to 52 W is due to alignment and HOM drifts.

had to be constantly available. Figure 5 shows an hourly sampled power trend over the time of O3 measured in PMC transmission at the LIGO site in Hanford. The PSL was operating reliable and the measured power decreased from 55 W to 52 W over the time of the observation run. This can be most probably explained by small alignment drifts in the optics that guided the front-end beam to the neoVAN-4S-HP. The imperfect alignment caused an increase in the neoVAN-4S's output mode. The additional HOM contribution was filtered out by the PMC and reduced the power in PMC transmission. Steps in the plot are due to realignment to the PMC, changes in the power offset for the power stabilization system as well as optimizations in the pump diode powers and temperatures for both amplifiers.

3. Pre-stabilized laser system for O4

In this section we will describe the pre-stabilized laser system that will be used for the next aLIGO observing run (O4). As mentioned in Section 2, a 180 W laser beam with a wavelength of 1064 nm going to the PMC was assumed to calculate the aLIGO design sensitivity. The PSL that was used

179   for O3 delivered 70 W before modecleaning. This was enough laser power for O3, but higher power
180   levels will be requested for the coming observing runs. Hence, a new system based on sequential
181   neoVAN-4S-HP solid state amplifiers, similar to the one presented in [18], was developed. This O4
182   laser system was designed to deliver an output power of 140 W before a pre-modecleaner, which
183   brings it closer to the aLIGO design value.
184   In the first part of this section we will point out the changes in the experimental setup compared to the
185   O3 PSL, which will be followed by a characterization of the O4 PSL prototype, performed in the test
186   and training facility at the aLIGO Livingston site.

187   *3.1. Setup*

188   The setup that will be used for O4 is presented in Figure 6. The seed laser source of the first
189   amplification stage is still a 2 W NPRO laser at a wavelength of 1064 nm. Its laser beam is then sent
190   through an EOM (EOM1) for sideband generation and phase actuation and a Faraday isolator (FI1) to
191   protect the NPRO from back reflections and back scattering. The laser beam transmitted by FI1 is
192   amplified by the first neoVAN-4S-HP. This amplifier is similar to the neoVAN-4S, but slighty different
193   dopings on the four Nd:YVO$_4$ crystals optimized for a pump wavelength of 878 nm and the usage of
194   Bragg grating stabilized pump diodes at a maximum output power of 65 W s the neoVAN-4S-HP to
195   produce a higher output power than the neoVAN-4S. A single neoVAN-4S-HP integrated in an aLIGO
196   reference system at the AEI in Hannover was already described and characterized [17]. 70 W of output
197   power from the first neoVAN-4S-HP was achieved with the system presented in this paper. It was
198   setup in the test and training facility at the LIGO Livingston observatory.
      The amplified laser beam is sent through FI2 and amplified by the second neoVAN-4S-HP to 140 W.
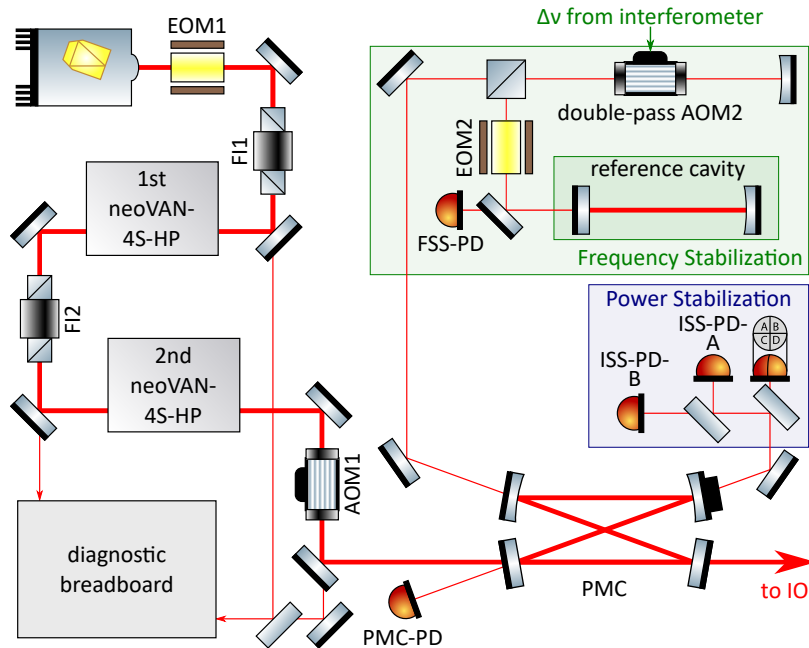

Figure 6. Simplified setup of the aLIGO O4 pre-stabilized laser system. A NPRO seeds two sequential
neoVAN-4S-HP amplifiers. The pre-stabilization concept is equal to the one used in O3.

199
200   This design is based on a successful test of two sequential neoVAN-4S-HP amplifiers at the AEI [18].
201   Similar to the O3 laser system, a DBB is used as characterization tool. A small fraction from the NPRO
202   beam, the beam amplified by the first neoVAN-4S-HP as well as the second neoVAN-4S-HP are sent
203   to the DBB. Electric shutters will be used here to control which beam is analyzed by the DBB. This
204   arrangement will allow a remote laser characterization while the gravitational wave detectors are
205   running.
206   The output from the second neoVAN-4S-HP is sent through AOM1 to the all-bolted PMC that was

already installed for O3 in Hanford as described in Section 2. The two PMC low power output
ports will be used for the frequency and intensity stabilization of the laser beam, in the same sensor
configuration as described in section 2 for the O3 system. The frequency pre-stabilization for the O4
system will be the same as for the O3 system described in Section 2.

A current shunt actuator similar to the one demonstrated in [17] is integrated in the neoVAN-4S-HP's.
This current shunt allows direct modulation the pump light and thus the neoVAN-4S-HP's output
power. Hence, the current shunt could replace AOM1 as actuator for the power stabilization. This
would bring the advantage to get rid of AOM1 as transmissive optic in the high power beam path [19].
On the other hand, changes in the diode current could also lead to changes in the beam parameters,
especially the RPN and HOM. Both options, the current shunt and the AOM were tested in the test
and training facility with similar results. For now it is decided to use the AOM, as the O4 baseline
actuator, as it showed a slight better low frequency behaviour compared to the current shunt and it
has shown its reliability in the last observing runs.

3.2. Characterization of the O4 laser system prototype

As previously mentioned, a first prototype of the O4 laser system as depicted in Figure 6 was
setup in the test and training facility at the LIGO site in Livingston, Louisiana. This prototype was
used to test and optimize the design and to gain experience with alignment, commissioning and
maintenance tasks without interfering with the operating gravitational wave detectors.
Here we will show the full characterization of the laser system before the frequency stabilization
subsystem (see green box in 6) was installed and before the power stabilization (blue box in 6) was
commissioned. All measurements were performed with the DBB as shown in Figure 6.
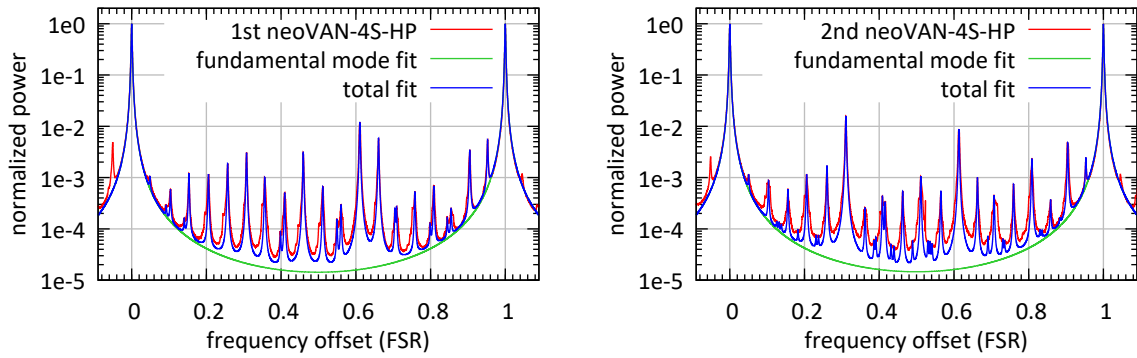Figure 7 shows modescan measurements of the laser beams after the first and second neoVAN-4S-HP

Figure 7. (a) Modescan of the laser beam amplified by the first neoVAN-4S-HP. The higher order mode
content of the laser beam was < 4.2%. (b) DBB modescan of laser beam amplified by the second
neoVAN-4S-HP. The higher order mode content of the laser beam was < 4.5%.

amplifier. The HOM peak at about 0.32 FSR increased after the second neoVAN-4S-HP. As explained
in Section 2, this peaks represents the TEM_{20} as well as TEM_{02} mode and can thus be explained by a
mode mismatching or astigmatism in the laser beam. The higher order mode content was measured to
be < 4.2% behind the first neoVAN-4S-HP and < 4.5% behind the second one. Hence, there are 134 W
in the TEM_{00} mode available.
The RPN measurements of the beams amplified by the first and second neoVAN-4S-HP, respectively,
are plotted as amplitude spectral densities in Figure 8. It has to be pointed out here that the NPRO
laser's noise eater was turned off in these measurements, whereas it was turned on in the RPN
measurements of the O3 laser, shown in section 2. The noise eater is a built-in power stabilization
integrated to suppress the NPRO laser's relaxation oscillation. It also suppressed The laser's RPN at
frequencies from about 10 Hz to several MHz as described in [9]. Additionally large fluctuations can
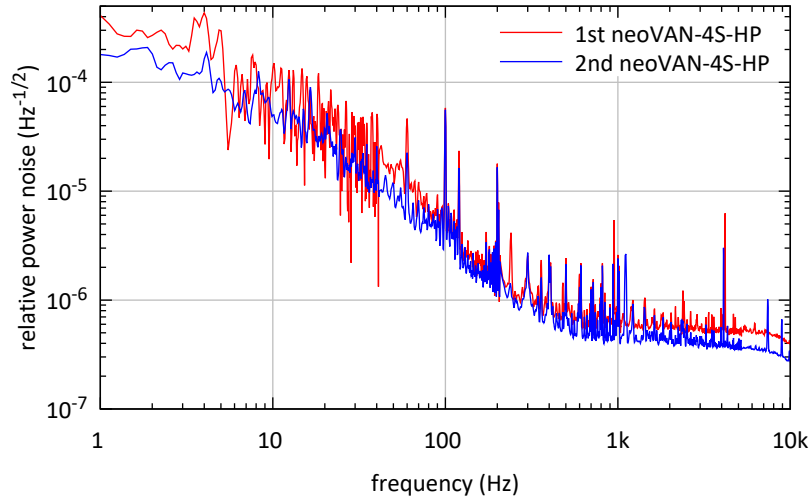
Figure 8. RPN measurements of the beam amplified by the first and second neoVAN-4S-HP, respectively.

be observed in the frequency band around 10 Hz, which were most probably caused by environmental disturbances. Besides that, the RPN measured behind the second neoVAN-4S-HP is decreased compared to its seed, which is the output of the first neoVAN-4S-HP. This behaviour is expected from a saturated amplifier with low noise pump diodes. If a certain seed power level is reached, the amplification is not linear anymore and a fixed power is added by the amplifier nearly independent of the seed power. The RPN of the amplifier's output beam is given by the uncorrelated sum of the seed and pump diodes relative power noise contributions. The pump diodes used for the neoVAN-4S-HP have much lower RPN as the amplifiers seed beam. Thus the output beam's RPN is equal to the seed RPN decreased by the inverse of the frequency dependent amplification, as described in [18].

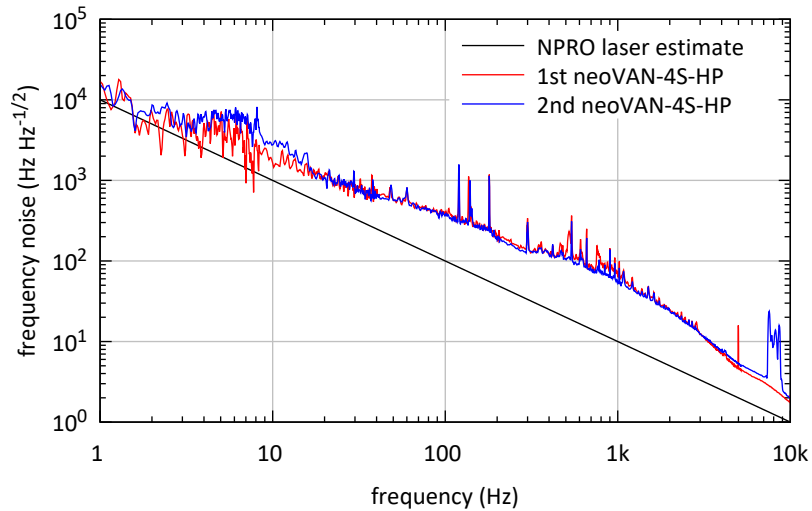Figure 9 shows the frequency noise measurements taken behind the two neoVAN-4S-HP amplifiers.

Figure 9. Frequency noise measurements of the beam amplified by the first and second neoVAN-4S-HP, respectively. Both curves are very close to each other and to the typical NPRO behaviour, as expected.

Both measurements show a similar noise level that is close to the expected NPRO noise. Fluctuations similar to the relative power noise can be observed around 10 Hz, which are expected to be caused by the same environmental issues.

It is important to note that the aLIGO laser room provides a much quieter environment than the test

255 and training laboratory. Hence, we expect that these low frequency fluctuations will be lower for laser
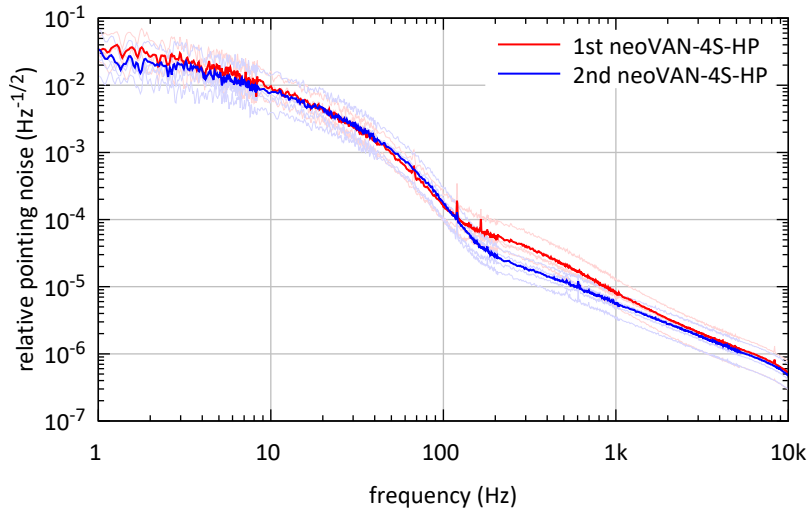systems installed in the observatory's laser rooms. The last DBB measurements taken for the setup

Figure 10. Relative beam pointing noise measurements of the beam amplified by the first and second
neoVAN-4S-HP, respectively.

256

257 show the relative beam pointing noise, measured behind each neoVAN-4S-HP, in Figure 10. The two
258 curves are close to each other, hence no additional noise was added by the second neoVAN-4S-HP.

259

4. Summary and Outlook

261 In this paper we present the PSL that was used for aLIGO's third observation run as well as the
262 PSL that will be used for O4. Both systems are based on solid state amplifiers that showed a high
263 reliability and a low noise behaviour.

264 The O3 PSL consisted of an eLIGO front-end together with a neoVAN-4S solid state amplifier. The
265 system delivered an output power of 70 W with a higher order mode content of $< 6.2\%$. The output
266 beam was spatially filtered by a bow-tie cavity and a frequency and power pre-stabilization was
267 performed. This system worked stably and reliably for the twelve month duration of O3.

268 The PSL that will be used for O4 consists of an NPRO laser and two neoVAN-4S-HP amplifiers in series.
269 A test setup showed an output power of 140 W with a higher order mode content of $< 4.5\%$. The laser
270 beam will be frequency and power stabilized just like the O3 system and a new pre-modecleaner will
271 be installed.

272 Further upgrades of aLIGO and future detectors will most likely require pre-stabilized laser systems
273 with even higher laser power and/or a longer wavelength. One option for more laser power would
274 be to continue to rely on the very stable and reliable neoVAN-4S-HP amplifiers and set them up in
275 series with a third amplifier, as similar presented in [18]. Here a three amplifier system with 195 W of
276 output power was presented. Another option would be to use high power fiber amplifier systems,
277 which were shown to work up to 200 W and above [20–22].

Conflicts of Interest: The authors declare no conflict of interest.

Abbreviations

The following abbreviations are used in this manuscript:

LIGO	laser interferometric gravitational wave observatory
eLIGO	enhanced LIGO
aLIGO	advanced LIGO
PSL	pre-stabilized laser system
NPRO	non-planar ring oscillator
O3	observation run three
O4	observation run four
DBB	diagnostic breadboard
QPD	quadrant photodiode
ASD	amplitude spectral density
EOM	electro-optical modulator
AOM	acousto-optical modulator
PMC	pre-modecleaner
IO	input optics
CDS	control and design system
HOM	higher order mode content
AEI	Albert Einstein Institute
RPN	relative power noise

References

1. LIGO Scientific Collaboration. Advanced LIGO. *Classical and Quantum Gravity* **2015**, *32*, 074001. doi:10.1088/0264-9381/32/7/074001.

2. Fricke, T.T.; Smith-Lefebvre, N.D.; Abbott, R.; Adhikari, R.; Dooley, K.L.; Evans, M.; Fritschel, P.; Frolov, V.V.; Kawabe, K.; Kissel, J.S.; Slagmolen, B.J.J.; Waldman, S.J. DC readout experiment in Enhanced LIGO. *Classical and Quantum Gravity* **2012**, *29*, 065005. doi:10.1088/0264-9381/29/6/065005.

3. Harry, G.M.; the LIGO Scientific Collaboration. Advanced LIGO: the next generation of gravitational wave detectors. *Classical and Quantum Gravity* **2010**, *27*, 084006. doi:10.1088/0264-9381/27/8/084006.

4. Kwee, P.; Bogan, C.; Danzmann, K.; Frede, M.; Kim, H.; King, P.; Põld, J.; Puncken, O.; Savage, R.L.; Seifert, F.; Wessels, P.; Winkelmann, L.; Willke, B. Stabilized high-power laser system for the gravitational wave detector advanced LIGO. *Optics Express* **2012**, *20*, 10617. doi:10.1364/oe.20.010617.

5. Winkelmann, L.; Puncken, O.; Kluzik, R.; Veltkamp, C.; Kwee, P.; Poeld, J.; Bogan, C.; Willke, B.; Frede, M.; Neumann, J.; Wessels, P.; Kracht, D. Injection-locked single-frequency laser with an output power of 220 W. *Applied Physics B* **2011**, *102*, 529–538. doi:10.1007/s00340-011-4411-9.

6. Kane, T.J.; Byer, R.L. Monolithic, unidirectional single-mode Nd:YAG ring laser. *Optics Letters* **1985**, *10*, 65. doi:10.1364/ol.10.000065.

7. Frede, M.; Schulz, B.; Wilhelm, R.; Kwee, P.; Seifert, F.; Willke, B.; Kracht, D. Fundamental mode, single-frequency laser amplifier for gravitational wave detectors. *Optics Express* **2007**, *15*, 459. doi:10.1364/oe.15.000459.

8. Adhikari, R.; Fritschel, P.; Waldman, S. Enhanced LIGO. Technical Report LIGO-T060156, LIGO Laboratory, 2006.

9. Kwee, P.; Seifert, F.; Willke, B.; Danzmann, K. Laser beam quality and pointing measurement with an optical resonator. *Review of Scientific Instruments* **2007**, *78*, 073103. doi:10.1063/1.2754400.

10. Kwee, P.; Willke, B. Automatic laser beam characterization of monolithic Nd:YAG nonplanar ring lasers. *Applied Optics* **2008**, *47*, 6022. doi:10.1364/ao.47.006022.

11. Morrison, E.; Meers, B.J.; Robertson, D.I.; Ward, H. Automatic alignment of optical interferometers. *Applied Optics* **1994**, *33*, 5041. doi:10.1364/ao.33.005041.

12. Põld, J.H. aLIGO bow-tie Pre-Modecleaner document. Technical Report LIGO-T0900616, Albert-Einstein-Institut Hannover, 2012.

13. Liu, J.; Savage, R.; King, P.; Zhang, L.; Appert, S. aLIGO all-bolted PMC. Technical Report LIGO-T1700543, LIGO Laboratory / LSC, 2017.

14. Mueller, C.L.; Arain, M.A.; Ciani, G.; DeRosa, R.T.; Effler, A.; Feldbaum, D.; Frolov, V.V.; Fulda, P.; Gleason, J.; Heintze, M.; Kawabe, K.; King, E.J.; Kokeyama, K.; Korth, W.Z.; Martin, R.M.; Mullavey, A.; Peold, J.; Quetschke, V.; Reitze, D.H.; Tanner, D.B.; Vorvick, C.; Williams, L.F.; Mueller, G. The advanced LIGO input optics. *Review of Scientific Instruments* **2016**, *87*, 014502. doi:10.1063/1.4936974.

15. Black, E.D. An introduction to Pound–Drever–Hall laser frequency stabilization. *American Journal of Physics* **2001**, *69*, 79–87. doi:10.1119/1.1286663.

16. Bork, R.; Hanks, J.; Barker, D.; Betzwieser, J.; Rollins, J.; Thorne, K.; von Reis, E. advligorts: The Advanced LIGO Real-Time Digital Control and Data Acquisition System. [2005.00219v2].

17. Thies, F.; Bode, N.; Oppermann, P.; Frede, M.; Schulz, B.; Willke, B. Nd:YVO4 high-power master oscillator power amplifier laser system for second-generation gravitational wave detectors. *Optics Letters* **2019**, *44*, 719. doi:10.1364/ol.44.000719.

18. Bode, N.; Meylahn, F.; Willke, B. Sequential high power laser amplifiers for gravitational wave detection. *Optics Express* **2020**. doi:10.1364/oe.401826.

19. Abbott, R.S.; King, P.J. Diode-pumped Nd:YAG laser intensity noise suppression using a current shunt. *Review of Scientific Instruments* **2001**, *72*, 1346. doi:10.1063/1.1334627.

20. Wellmann, F.; Steinke, M.; Meylahn, F.; Bode, N.; Willke, B.; Overmeyer, L.; Neumann, J.; Kracht, D. High power, single-frequency, monolithic fiber amplifier for the next generation of gravitational wave detectors. *Optics Express* **2019**, *27*, 28523. doi:10.1364/oe.27.028523.

21. Wellmann, F.; Steinke, M.; Wessels, P.; Bode, N.; Meylahn, F.; Willke, B.; Overmeyer, L.; Neumann, J.; Kracht, D. Performance study of a high-power single-frequency fiber amplifier architecture for gravitational wave detectors. *Applied Optics* **2020**, *59*, 7945. doi:10.1364/ao.401048.

22. Zhao, J.; Guiraud, G.; Pierre, C.; Floissat, F.; Casanova, A.; Hreibi, A.; Chaibi, W.; Traynor, N.; Boullet, J.; Santarelli, G. High-power all-fiber ultra-low noise laser. *Applied Physics B* **2018**, *124*. doi:10.1007/s00340-018-6989-7.